Pergamon

PII: S0042-6989(96)00150-2

Vision Res., Vol. 36, No. 24, pp. 3969–3985, 1996

Printed in Great Britain
0042-6989/96 $15.00 + 0.00

Gain Control and Hyperpolarization Level in Cat Horizontal Cells as a Function of Light and Dark Adaptation*

W. A. van de GRIND,† M. J. M. LANKHEET,† R. J. A. van WEZEL,† M. H. ROWE,‡ J. HULLEMAN§

First a model is presented that accurately summarizes the dynamic properties of cat horizontal (H-) cells under photopic conditions as measured in our previous work. The model predicts that asymmetries in response to dark as compared to light flashes are flash-duration dependent. This somewhat surprising prediction is tested and confirmed in intracellular recordings from the optically intact *in vivo* eye of the cat (Experiment 1). The model implies that the gain of H-cells should be related rather directly to the sustained (baseline) membrane potential. We performed three additional experiments to test this idea. Experiment 2 concerns response vs intensity (*R–I*-) curves for various flash-diameters and background-sizes with background luminance varying over a 4 log unit range. Results support the assumption of a rather strict coupling between flash sensitivity (gain) and the sustained level of hyperpolarization. In Experiment 3 we investigate this relation for both dark and light flashes given on each of four background light levels. The results suggest that there are fixed minimum and maximum hyperpolarization levels, and that the baseline hyperpolarization for a given illumination thus also sets the available range for dark and light flash-responses. The question then arises whether, or how this changes during dark adaptation, when the rod contribution to H-cell responses gradually increases. The fourth experiment therefore studies the relationship between gain and hyperpolarization level during prolonged dark-adaptation. The results show that the rod contribution increases the polarization range of H-cells, but that the gain and polarization level nevertheless remain directly coupled. H-cell models relying on a close coupling between polarization level and gain thus remain attractive options. Copyright © 1996 Elsevier Science Ltd.

Horizontal cells Cat retina Rod–cone interaction Dark adaptation Light adaptation

INTRODUCTION

In the 38 years since the first intracellular recordings from mammalian (cat) horizontal cells (H-cells) by Grüsser (1957) and by Motokawa *et al.* (1957) an impressive body of knowledge has been established about the morphology and light responses of these cells. The tradition of studying H-cells in lower vertebrates is only 4 yr older [Svaetichin (1953); who like Grüsser, and like Motokawa *et al.*, initially assumed that he was recording from receptors] and has led to an even more extensive literature. Yet uncertainty about the functional role of these cells still remains. Many accept the idea that H-cells in all vertebrates are responsible for the surround component of ganglion cell (G-cell) receptive fields (RFs), and evidence in favour of this idea has been presented [e.g. for poikilothermic animals Werblin & Dowling (1969); Naka (1971, 1977); Naka & Nye (1971); Naka & Witkovsky (1972); and in a mammalian retina Mangel & Miller (1987); Mangel (1991)]. Reports on the absence of a surround component in many cat bipolar (B-) cells (Nelson *et al.*, 1981; Nelson & Kolb, 1983; Kolb & Nelson, 1984) on the other hand have cast doubt on such a role for H-cells in contrast vision, at least in mammals. For example, Weber and Stanford (1994, p. 498) state "that the surround component of cat retinal ganglion cell RFs may be generated in the IPL by amacrine cell input". Troy *et al.* (1993) recently quantified the properties of Y-type G-cell centre and surround as a function of ambient illumination and found surround diameters of some 7.5 deg, which they assume to be a sign of active surround-signal transport by amacrine cells. Many models of G-cell function work without H-cells [e.g. Gaudiano (1994)]. Moreover, recent authoritative reviews on the rod-pathway scarcely

*This paper is dedicated to the memory of O.-J. Grüsser, a pioneer in neuroscience.

†Neuroethology Group, Helmholtz Institute and Comparative Physiology, Universiteit Utrecht, Padualaan 8, 3584 CH Utrecht, The Netherlands.

‡Department of Biological Sciences, Neurobiology Program, Ohio University, Athens, Georgia, U.S.A.

§Nijmegen Institute for Cognition and Information, University of Nijmegen, Nijmegen, The Netherlands.

mention the B-type H-cell axon terminal (HBAT) and do not explicitly grant it a role in rod vision (Daw *et al.*, 1990; Wässle *et al.*, 1991). Yet it is our guess that H-cells and their axon terminal processes play an important role in vision. Weighing the evidence we still favour the idea that H-cells and their axon terminals (ATs) play an important role in structuring the G-cell (and B-cell) surround and thus have a function in contrast vision (see the Discussion).

Inspired by Grüsser (1957) a new approach was developed in 1971 in Grüsser's laboratory enabling recordings from the optically intact *in vivo* eye (van de Grind *et al.*, 1973; Foerster *et al.*, 1973, 1977a,b; van de Grind, 1981; van de Grind & Grüsser, 1981). Since then a number of technical improvements developed in our own laboratory [e.g. Molenaar & van de Grind (1980)] and elsewhere [e.g. Brown & Flaming (1977)] have enabled us to obtain increasingly stable intracellular recordings from H-cells and G-cells in the retina of the optically intact *in vivo* eye of the cat [for early work see: Molenaar & van de Grind (1979a,b); Molenaar *et al.* (1983)]. In a recent series of dark adaptation experiments, for example, some H-cells were held for many hours without any change of properties and without a trace of DC-drift. Thus even the sustained polarization level could be measured reliably and reproducibly as a function of background light and adaptation level, a topic to be discussed below. In this set-up it has also proved possible to obtain very stable intracellular G-cell recordings from the optically intact *in vivo* eye of the cat (Lankheet *et al.*, 1989a,b; Przybyszewski *et al.*, 1993, 1995). The present report is one of a series in which we extensively studied the light adaptation properties of H-cells in the cat (Lankheet *et al.*, 1991a, 1993a,b) and their dark adaptation (Lankheet *et al.*, 1996a,b). We have shown previously (Lankheet *et al.*, 1990, 1992) that the spatial properties of H-cells in the light-adapted retina are highly similar to those of G-cell RF surrounds in photopic/mesopic vision. Among other things our new results show that H-cell soma responses from both A-type (HA-) and B-type (HB-) horizontal cells still have a strong cone-component after 45 min of dark adaptation and that their lowest thresholds to light flashes after prolonged dark adaptation are at least 2 log units above those of G-cell centres. Thus HA- and HB-cell bodies do not seem to play a prominent role in scotopic vision. We have also obtained evidence that the temporal and spatial properties of HA- and HB-cells change significantly (roughly a factor of two) during dark adaptation (Lankheet *et al.*, 1996a,b). Such data allow a critical evaluation of the hypothesis that H-cells make up the G-cell surrounds.

To the extent that G-cells still have a surround in the fully dark-adapted state this surround component should travel another route, viz. from rods through the HBAT and rod bipolars, or it might be structured in the proximal retina (Frishman & Sieving, 1995). If HBATs are not involved in this scotopic centre–surround process the only alternative role we see for them at the moment is to take care of rod network-adaptation. This should in principle be deducible from their sensitivity and RF-size as a function of the state of adaptation. However, HBATs [the functional H_n-type of Foerster *et al.* (1977a,b)] are harder to record from and especially to keep stable for prolonged dark adaptation sessions than the H-cell bodies. We only have preliminary results for HBATs so far and will not discuss them here in any detail. This paper concentrates on HA- and HB-cell *bodies*. Of course, in cases where we discuss "rod components" of H-cell soma-responses these components might implicitly include network-feedback control of rods by HBATs. In any case these rod components are assumed to enter the H-cell bodies via cones (Nelson, 1977), so we will start with results on the cone-H-cell network (Experiments 1–3) before considering the rod contribution in more detail.

It is usually an asset if one can summarize extensive data sets sufficiently accurately with a simple model. We developed such a model to summarize the data on H-cell dynamics as a function of the state of light adaptation. It is an improved version of a model described previously (Lankheet *et al.*, 1993b), and does not yet include spatial properties and their changes with adaptation, nor the rod-contribution. Among other things the model suggests that the amount of asymmetry between responses to dark flashes and light flashes depends upon the background luminance and, perhaps more surprisingly, especially upon the flash duration. As described below, we checked these predictions with intracellular H-cell recordings (Experiment 1) and found them to be correct. An important question generated by our modelling attempts is which physiological variable(s) control(s) sensitivity. One candidate is the sustained (baseline) component of the H-cell membrane potential, which we will call the "hyperpolarization level" for short. Thus, it is important to quantify its relation to sensitivity and dynamics of, for example, superimposed flash responses. It proves that there is a close coupling between gain (flash sensitivity) and hyperpolarization level (Experiment 2) and the latter variable also determines the voltage range available to dark and light flash responses (Experiment 3). In these experiments the conditions were such that cones strongly dominated the H-cell responses. However, also rod signals can reach the H-cell somata through the gap junctions with cones and the cone-to-H-cell synapse. This rod contribution was studied in Experiment 4. It increases during dark adaptation and in fact only becomes significant in most H-cell bodies below the upper or middle part of the mesopic range of luminances. Interestingly the available voltage range for H-cell soma-responses increases in parallel with an increasing rod contribution for a while until it reaches a new upper level, the rod+cone range. Even in this extended range we find that the close coupling between gain and hyperpolarization level remains intact. The present new findings and those of the companion papers (Lankheet *et al.*, 1996a,b) provide some of the boundary conditions for a more complete model of H-cell functioning in the cat retina, to be developed in the near future.

METHODS

Terminology

By sheer coincidence all major cell classes of the retina have names starting with a different letter: R = rod; C = cone; H = horizontal cell; B = bipolar cell; G = ganglion cell; A = amacrine cell; I = interplexiform cell; M = Müller cell; E = epithelial cell. It would be a shame not to use this natural order of things and thus we always start abbreviations for cell types with this major class designation. This can be followed by subdivision letters or numbers, where we follow the literature as far as feasible and use capital and/or Greek letters for morphological classification. An index and/or lower case letter is proposed for functional classifications. For example, A and B type H-cells become HA and HB, the latter cell's axon terminal HBAT, but narrow bandwidth or medium bandwidth H-cells would be H_n and H_m (Foerster *et al.*, 1977a,b). We are not in favour of arbitrary acronyms like HBC for hyperpolarizing bipolar cell, since one always has to guess which letter happens to stand for the major cell type. A rigid convention is preferable and the least we can do is to follow one ourselves.

Simulation methods

The simulations were programmed in Turbo Pascal 6.0 (Borland International) installed on a Mitac IBM-compatible PC equipped with a numerical co-processor. The values of the parameters were chosen in such a way that the input could be expressed in cd/m^2 and that the output would be in mV. This allowed a direct comparison of simulation results and intracellular measurements. The discrete time steps setting the temporal grain of the simulation were always at least a factor of one hundred finer in simulated time than the shortest time constant of the model. The results have been independently reproduced in later simulations in Matlab on a Power Macintosh.

Electrophysiological methods

The methods of recording, light stimulation and data analysis have been described in detail elsewhere [e.g. Lankheet *et al.* (1990, 1996a)]. Briefly, the femoral artery and vein, as well as the trachea were cannulated under pentobarbital anesthesia (40 mg/kg body wt) and the cat, wrapped in a heating blanket was placed in a specially designed stereotaxic device (Molenaar & van de Grind, 1980) after treating all wounds and pressure points with a local anesthetic (2% Lidocaine). Paralysis was initiated with 80 mg gallamine triethiodide (Flaxedil) and maintained with a continuous infusion containing 6 mg Flaxedil per kg per hour, while artificial ventilation was adjusted when necessary to maintain the end-tidal CO_2 at about 4.0%. Rectal temperature was kept at about 38°C. The continuous infusion of a 5% Ringer solution (6 ml/hr) contained the Flaxedil, glucose and 3 mg Nembutal per kg per hr. Additional doses of anesthetic were administered whenever necessary as judged from the heart rate and blood pressure (including pressure waves in the lower aorta, measured via the femoral artery). Atropine and phenylephrine eye drops were used to dilate the pupils and retract the nictitating membrane. The eye was fixed with sutures around the limbus to a metal eye ring connected to the stereotaxic frame and the whole cornea was covered by a light-tight (metal-covered) scleral contact lens with a vertical slit aperture (artificial pupil) of 1.5 mm × 6 mm. To prevent loss of corneal transparency the contact lenses were frequently removed to clean the cornea with a slightly hypertonic Ringer solution. Micropipettes were pulled to a tip diameter well below 0.2 μm, backfilled with 4 M potassium acetate [in some cases HRP was added as well, see Lankheet *et al.* (1996a)], and usually had an impedance at 1000 Hz of 15–60 MΩ. Apart from signal monitoring and provisional on-line analysis, the amplified cell responses were also stored on a digital tape recorder with a pass band from DC to 12 kHz for later, more detailed, off-line analysis. Two 450 W xenon light sources were controlled by 450 W modulatable power amplifiers (Heinzinger, 0–1000 Hz, 0–90% modulation). Their condensed (parallel) light bundles were projected through separate optic channels containing (where appropriate) neutral density filters, electronic shutters, filter wheels, narrow-band interference filters and the like. The optic channels were combined in a half-silvered mirror and projected via a mechanical oscilloscope system (Molenaar *et al.*, 1980) on a tangent back-projection screen placed at 57 cm from the cat's eye. The screen subtended 80 × 80 deg at the cat's eye. After eye preparation and before the first recording session an image of the optic disk and retinal blood vessels was back-projected on the screen and traced on drawing paper covering the screen in a precisely standardized way. Whenever appropriate during the experiment we checked the positioning of the eye with the help of this drawing and plotted measured RFs on it. Also the optical quality of the cat's eye and refraction were checked regularly. If necessary refraction was corrected with spectacle lenses. We searched for H-cells with squarewave modulated flicker stimuli of a photopic luminance and after impalement determined basic characteristics like RF-position, RF-size, flicker fusion frequency for a number of spot sizes and light colours, etc. All stimulus parameters (e.g. of the filter wheels, shutters, mechanical oscilloscope and light source amplifiers) were under computer control, allowing complete measurement series to be fully preprogrammed. Intervention and redirection of measurements was always possible on the basis of the on-line analysis appearing on the computer screen together with all stimulus details.

RESULTS

Model of cone-dominated H-cell dynamics

Light and dark adaptation can be viewed as gain control, where an input signal x is multiplied by a light-level-dependent gain factor g, or alternatively divided by a scaling factor s, to obtain an output y: thus

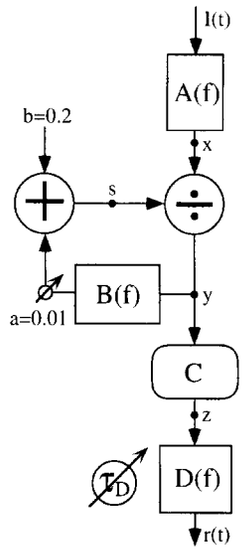

FIGURE 1. Dynamic model of a cone-dominated H-cell. Low-pass filter $A(f)$ consists of four stages in the old and two stages in the revised model. The stages have RC-time constants of about 7 msec. $B(f)$ is a single-stage low-pass filter (leaky integrator) with a long time constant of 250 msec. C is a non-linear compression stage described by $z = z_{max}\, y^n/(y^n + \sigma^n)$, with $z_{max} = 35$, $\sigma = 200$, and $n = 0.85$. The final filter $D(f)$ consisted of two low-pass stages with RC constants of 4 and 6 msec in the old model. In the new model the latter low-pass end-stage is preceded by a three-stage low-pass filter with equal (but variable) time constants τ_D, which are controlled by signal z via a leaky integrator with RC time of 250 msec. The leaky-integrated signal $\langle z \rangle$ is an estimate of the average value of z and thus of log average luminance. The control is defined by $\tau_D = \tau_1 - k_1 \langle z \rangle$ msec, with $\langle z \rangle$ in mV and the constants as given in the text. It is symbolized by the arrow-crossed circle to the left of the corresponding filter box. The constants a and b of the scale-factor feedback-loop have the indicated fixed values.

$y = g \cdot x = x/s$ [e.g. Bouman & Ampt (1966); Rushton (1965, 1972)]. There are two simple options, namely a feedforward gain control in which s is made proportional to the average input signal $\langle x \rangle$, or a feedback control system where s is made proportional to the average output signal $\langle y \rangle$. In both cases the addition to the scale factor of a nonzero constant b prevents division by zero. These two options lead to Weber-type and deVries–Rose (= square-root) type of gain control, respectively [van de Grind *et al.* (1971); reviews in van de Grind *et al.* (1973); and Bouman *et al.* (1985)]. Recently Lankheet *et al.* (1993b) found that the feedback scaler (de Vries–Rose mechanism) followed by a static compression C was an excellent basis for a model mimicking the dynamic properties of cat cone-dominated H-cells. The model is schematized in Fig. 1.

The model consists of a multistage low-pass filter $A(f)$ representing the filtering properties of outer segments of the dominant L-cones (555–560 nm), followed by a feedback scaler with a low pass filter $B(f)$ in the feedback loop, a static compression C (where $z = z_{max} y^n/(y^n + \sigma^n)$ with $z_{max} = 35$ mV, $\sigma = 200$, $n = 0.85$) and a final multistage low-pass filter D. The threshold vs intensity (T–I) curves of H-cells can only be mimicked well if the static nonlinearity C *follows* the feedback scaler. The scaler's feedback low-pass filter provides an estimate of the average output $\langle y \rangle$ which is weighted by constant $a = 0.01$ and added to a constant $b = 0.2$ at the summation point, which leads to the scale-factor setting at the division operator. The final filterbox D in Fig. 1 contained a (sign-inverting) low-pass filter of one or two stages and is the part of the model that we now wish to modify, as explained below. The original model successfully mimicked H-cell cone-dominated responses to flashes and sinewave flicker. The waveform of the flash-response, flash response vs intensity (R–I) curves and their horizontal shift with background intensity, sinewave flicker responses and their harmonic distortion were all mimicked extremely well, both qualitatively and quantitatively [see Lankheet *et al.* (1993b)].

The model had one weakness, namely that the high-frequency flicker-response amplitudes changed with background intensity in the model, but not in the H-cell responses. This can be remedied by choosing different time constant values for different background luminances. For example, if the time constants of filter $A(f)$ are made equal to $\tau_A = \tau_0 - k_0 * \mathrm{Log}\langle L \rangle)$ the desired results are readily obtained. Here $\langle L \rangle$ is the mean luminance in cd/m^2, $\tau_0 = 13.5$ msec and $k_0 = 4.25$ msec/(cd/m^2). It is unsatisfactory, however, to have a parameter follow the log light level without specifying how this could be implemented. Fortunately, the idea translates rather directly into a change of the time constants of filter $D(f)$ by the average output signal z of the compression box, since the average output is roughly proportional to average log light intensity. Thus $\tau_D = \tau_1 - k_1 * \langle z \rangle$, where $\langle z \rangle$ is the estimated average value of z in mV, works very well. Here $\tau_1 = 11.5$ msec and $k_0 = 0.5$ msec/mV. We implemented this idea in the simulation by sending z through a low pass filter (leaky integrator) with a long time constant of 250 msec to produce $\langle z \rangle$. In the old model, filter D consisted of two low pass filters in series with time constants of 6 and 4 msec. The latter filter is replaced in the new model by a three-stage low-pass filter, the time constants of which are equal and controlled by $\langle z \rangle$ according to the previous formula. In order not to get too large a phase shift in sinewave responses this necessitated a modification in $A(f)$, where two of the four low-pass filters are removed. It should be emphasized that the manipulations with the linear filters are not very essential to the principles involved. There is quite some freedom in shifting them between stages, even though this influences the optimal parameter settings of the other components.

Two other simplifications in the original as well as the modified model that are not essential to our present purposes should nevertheless be noted. In the first place we left out the second-order filter, proposed by Foerster *et al.* (1977a) as an explanation of the 35–40 Hz oscillations that are so often seen in H-cell responses (*op. cit.*). This component can be added if desired (at the cost of two single stage low-pass filters) to explain such oscillations. However, for the time being we ignore the oscillations, which are not very prominent for the light regimes under

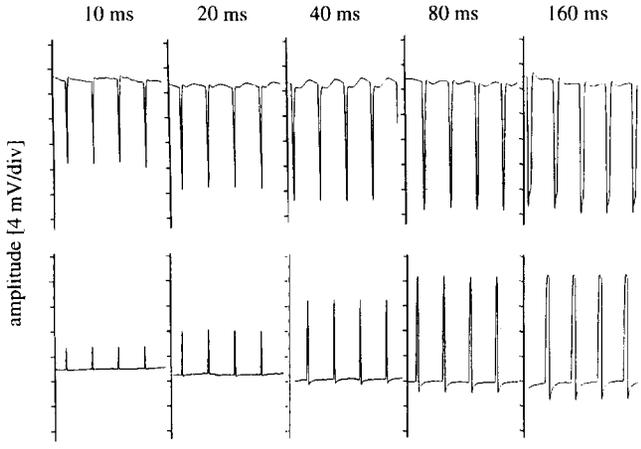

FIGURE 2. Light and dark flash responses as a function of flash duration, recorded intracellularly from a cone-dominated H-cell. Light flashes were given on a steady background of 0.01 cd/m^2 and reached a maximum luminance of 1500 cd/m^2, whereas dark flashes were given in the opposite direction between the same luminance levels. The flash-durations are indicated above the light-flash responses in the upper row and also hold for the dark-flash responses of the bottom row.

present discussion. The second simplification is that we concentrate on one receptor type, the dominant L cone (555–560 nm). Foerster *et al.* (1977a) have shown how the influence of other cone-types and rods can be taken into account. When we describe the process of dark adaptation, where the rods start to contribute significantly to H-cell responses, we will treat the problem of taking rod influences into account (Experiment 4).

The addition of time-constant control indeed rectified the main shortcoming of the previous model, without destroying its strong points. Therefore, we can refer to the results for the old model (Lankheet *et al.*, 1993b) rather than recapitulate them here. The main change is indeed that the discrepancy between the H-cell results in Fig. 7(A) of Lankheet *et al.* (1993b) and the simulation results of Fig. 11(A) (*op. cit.*) has been eliminated. In other words, for the new model the high-frequency flicker–response amplitudes are independent of background level, as required by the H-cell data. This is of course a rather trivial result, because it is exactly what the modification was all about. Here we prefer to describe a new experimental test of the improved model based on measurements of the asymmetry between an H-cell response to a light flash from level 1 to 2 and dark flash from level 2 to 1.

Experiment 1

This experiment was suggested to us by some surprising results of the model simulations and thus conceived as a test of the model. For simplicity of presentation we describe it in reverse, that is first the H-cell results and then the model simulations. In the experiment two luminance values are of importance—let us call them L_1 and L_2 with $L_1 > L_2$. If a spot is kept at a steady luminance level L_2 for a while and then briefly flashed to L_1 we have a light flash, if we similarly flash from steady level L_1 to L_2 we have a dark flash. Figure 2 shows the type of results one gets in such an experiment on H-cells. Here L_1 was 1500 cd/m^2 and L_2 was 0.01 cd/m^2. It is immediately obvious from Fig. 2 that short light flashes provoke a larger response than short dark flashes, but that the difference decreases for increasing flash duration.

The model predicted this result quite well both qualitatively and quantitatively (Fig. 3), and also enabled us to understand the influence of the flash-duration. There is a simple explanation for asymmetry in terms of the model of Fig. 1. When a light flash is turned on from a very low luminance background (e.g. 0.01 cd/m^2) the initial value of the scale factor is low (here 0.2, a gain factor of 5), so there will be an amplified initial response. After the initial transient the low-pass filter (B) in the feedback loop will start to charge and the response will be scaled down to a lower sustained level. Hence the transient character of the initial hyperpolarizing response to longer lasting light flashes. The dynamic gain adjustment does not influence the flash-response amplitude (initial transient) in this case. For very brief flashes filter A (low-pass) will limit the amplitude, but this will occur equally for light and dark flashes. For dark flashes, however, we start at a high light level (e.g. 1500 cd/m^2) so the gain will be low (filter B adds its steady output to the scale factor). The dark flash responses (high to low) will thus be smaller than the light flash responses (low to high), especially for brief flashes, where there is no time to adjust the scale factor through the slow filter B. If the dark flashes last longer, there will be a dynamic upward adjustment of the gain factor during the flash. Their amplitude will therefore increase with flash duration because of two factors:

1. Disappearance of the influence of filter A on the amplitude (which occurs equally for light flashes); and
2. The dynamic upward adjustment of the gain during the flash.

Figure 3 presents a comparison of results for an H-cell [Fig. 3(B): cell 91-101, the same as in Fig. 2] and for the model [Fig. 3(C), from model-responses such as those in Fig. 3(A)]. The graphs of response-amplitude vs flash-duration show how well the model predicts the measurements. We did not optimise the model parameters to improve the fit in Fig. 3, since the parameters were fixed beforehand by fitting previous results (Lankheet *et al.*, 1993b).

An explicit model like the one in Fig. 1 has the advantage that it generates specific predictions that can be tested empirically. If the control of scale factor and time constants indeed occurs as suggested by the scheme in Fig. 1, the controlling variables are expected to be baseline (sustained) polarization levels. Thus the question arises, whether (and if, how) the sustained voltage levels of H-cells relate to the gain settings or, for example, to the temporal properties and their control. If one can prove that there is no relation of this sort one has falsified the type of modelling approach illustrated in Fig.

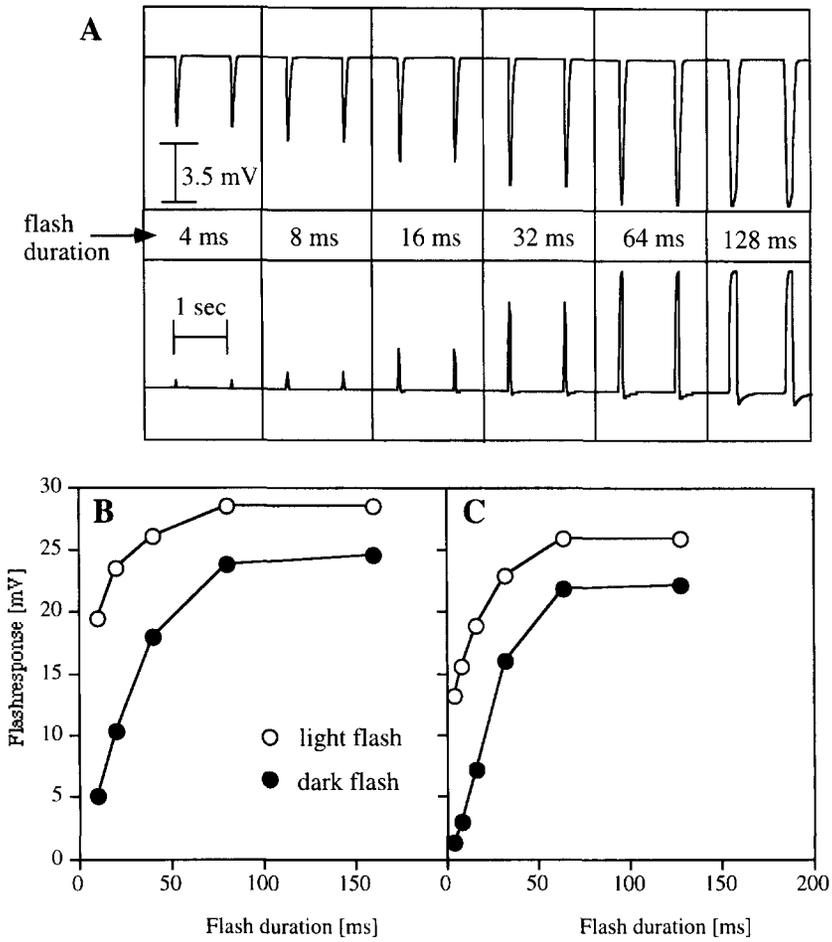

FIGURE 3. Upper row in (A): responses of the model of Fig. 1 to light flashes with a maximum luminance (background included) of 1500 cd/m^2 given on a steady background of 0.01 cd/m^2. Bottom row in (A): model responses to dark flashes going briefly from the steady background value of 1500 cd/m^2 to a level of 0.01 cd/m^2. The centre row in (A) gives the values of the flash durations for the various responses. These model responses can be compared directly to the intracellular H-cell recordings of Fig. 2, which were obtained for the same type of flashes between the same luminance levels. To enable a more quantitative comparison the graphs in (B) and (C) give the corresponding results for a H-cell [(B) the cell of Fig. 2] and the model (C). Apart from a vertical shift of a few mV (which might stem from the small contribution of rods in the H-cell response) the results of model and cell are virtually identical. All model parameters were fixed *a priori* as described in the text and legend of Fig. 1 and were not optimized in any way to improve the fit of the simulation results to the data. The phenomenon of asymmetry between dark and light flashes is explained in the text.

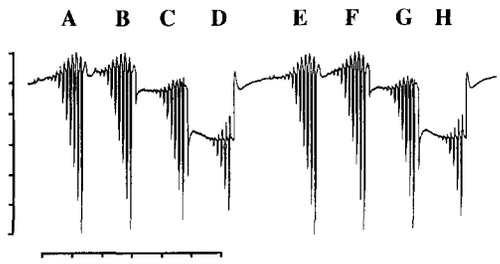

FIGURE 4. Part of a recording trace that illustrates the protocol for measuring response vs intensity (*R–I*) curves on different backgrounds. The time calibration is 10 sec per division, the potential calibration is 4 mV per division. The background spot in this case was 4.3 deg in (A–D) and 3.1 deg in the second part of the recording (E–H). The intensity of the background spot was changed from letter to letter in the sequence −3 log units (A and E), −2 log units (B and F), −1 log units (C and G) and 0 log units (D and H), where 0 log units corresponds to 170 cd/m^2. A flash series with increasing flash intensity was started a few seconds after each background-change. The test flashes were 1.1 deg in diameter and lasted 400 msec, while their intensity increased from flash to flash in 0.4 log unit steps until the highest luminance (0 log units of the flash channel) was reached, which corresponded to 1500 cd/m^2. Cell 92-101.

1. This is the purpose of the next two experiments. Conversely, if there *is* a direct relation between baseline polarization level and flash threshold or sensitivity, that does not necessarily support the type of model of Fig. 1. However, such a result invites further critical tests and model development, as will be discussed further on.

Experiment 2

In this experiment flash-response vs flash-intensity (*R–I*) curves were measured on various background levels, for various flash-diameters as well as background spot-sizes. An example of a recording is presented in Fig. 4 to clarify the experimental protocol.

In the recording of Fig. 4 the background spot had a diameter of 4.3 deg for the period from A–D and 3.1 deg for the period E–H. The four series of flashes in each case (A–D and E–H) were given superimposed on background spots of increasing intensity: −3 log units (A and E), −2 log units (B and F), −1 log units (C and G) and

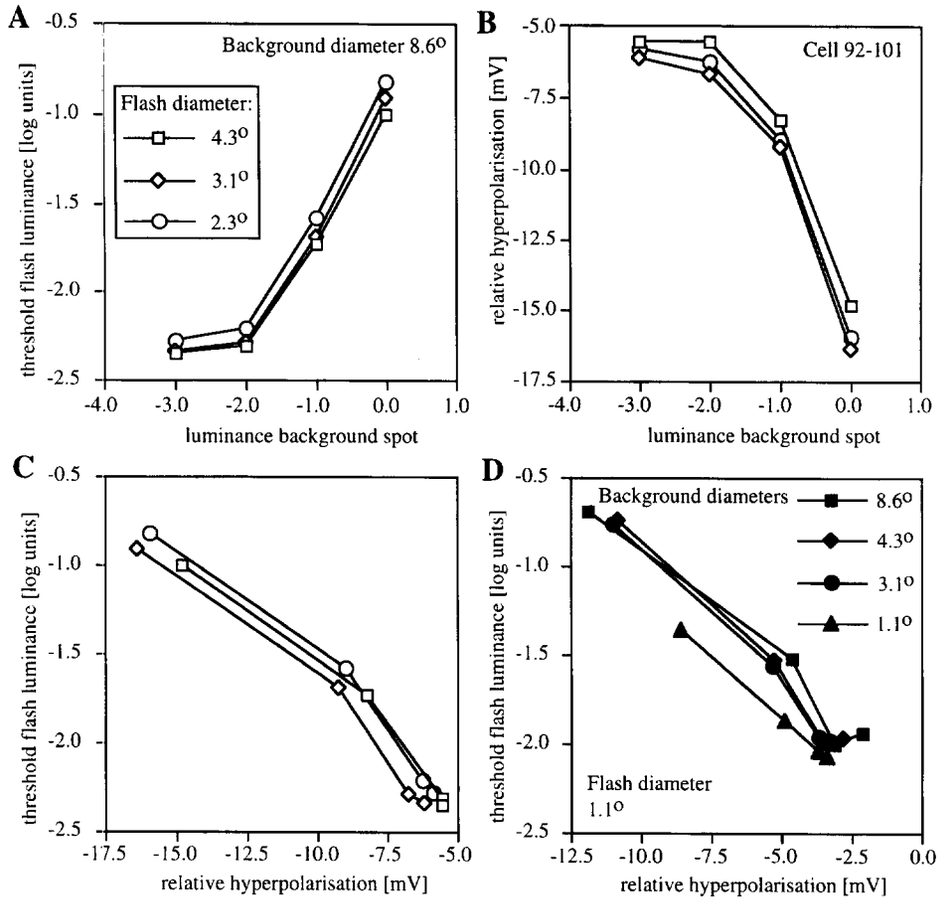

FIGURE 5. The relationship between increment threshold, hyperpolarization level and background luminance. (A) Presents threshold-flash luminance, for a 2 mV threshold-criterion, plotted against background luminance in log units, where 0 log units corresponds to 170 cd/m^2. Here, as in (B and C), the background spot diameter is constant and equal to 8.6 deg, while the different symbols refer to different flash diameters as indicated in the figure. The legend in (A) also holds for (B and C). (B) presents the hyperpolarization level of the H-cell in mV as a function of background luminance. Since we do not know the absolute potential value at the start of the cell-recording, the hyperpolarization values are only known up to an additive constant [arbitrary vertical shift in (B), but identical for all measured curves]. (C and D) summarize the relation between hyperpolarization level and flash threshold. In (C) this is done for a large background spot and the same three flash diameters as for (A) and (B). As expected it shows only a slight influence of flash size. In (D) the situation is different, since now the background diameter is changed in a few steps from a large (8.6 deg) to a small (1.1 deg) value and is thus expected to influence the flash-threshold less and less. This expectation is borne out. Cell 92-101.

0 log units (D and H), where 0 log units corresponded to 170 cd/m^2. Each flash series consisted of small flashes of 1.1 deg dia, the luminance of which increased in 0.4 log unit steps from flash to flash (maximum 1500 cd/m^2). The resulting *R–I* curves have partly been reported previously (Lankheet *et al.*, 1991a, 1993a,b). Here we wish to concentrate on the hyperpolarization level, which can be determined at, say, 5 sec after the change to a different background luminance. It can be seen in this example, that this baseline hyperpolarization level is very stable, even during a series of flashes of increasing intensity. Figure 4 clearly shows that the strongest change in polarization level occurs for the last step from -1 to 0 log units intensity, the weakest for the first step from -3 to -2 log units. Such a nonlinear relation between log luminance and membrane polarization is to be expected from the model of Fig. 1. If the sustained component of the H-cell membrane potential is involved in the control of sensitivity, one would expect parallel changes between sensitivity and sustained response. Of course such a relation does not *prove* an involvement of the H-cell membrane potential in sensitivity control, since sensitivity and sustained component could have a common cause, e.g. in the receptors or their end feet. Nevertheless it is of interest to study the relationship, which is illustrated in Fig. 5 for one H-cell. Results for seven other cells that had similarly stable sustained levels were virtually identical except for small differences in the total voltage range (which might depend upon the recording locus in the cell) or the absolute position of the threshold curve along the flash-luminance axis.

Figure 5(A) shows the threshold luminance for flashes of three different diameters (4.3, 3.1 and 2.3 deg) on a background spot of 8.6 deg dia, as a function of the luminance of the background spot. Figure 5(B) presents the hyperpolarization level as a function of this same background luminance. The form of the curve in Fig.

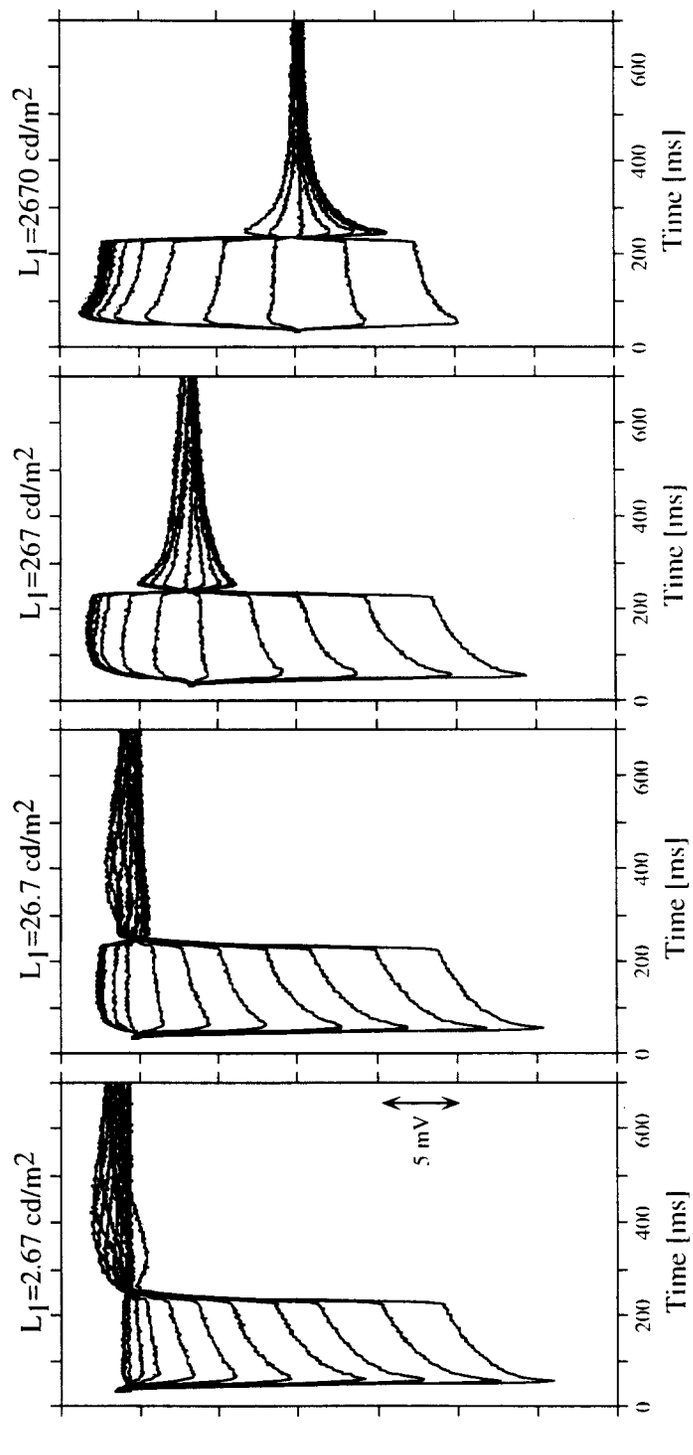

FIGURE 6. Superimposed H-cell responses to dark and light flashes (dia 3.1 deg) generated by briefly (200 msec) exchanging the equal-diameter test and background spots. Background luminances are indicated above the panels. The flash luminances were decreased in steps of 0.4 log units (factor of 0.398) from a maximum of 15900 cd/m^2 and the flash was therefore a "dark" flash if its luminance was lower than the background luminance that it briefly replaced. A RAE is seen only for the strongest flashes on the lowest backgrounds. This H-cell is clearly cone-dominated. Dark and light flash responses are more nearly symmetrical on the higher background luminances. For lower luminance backgrounds there is hardly any scope for dark responses, since there appears to be a rather rigid low-hyperpolarization limit (upwards direction in this figure). Note the shift of the hyperpolarization level with background luminance and its independence of the flash parameters.

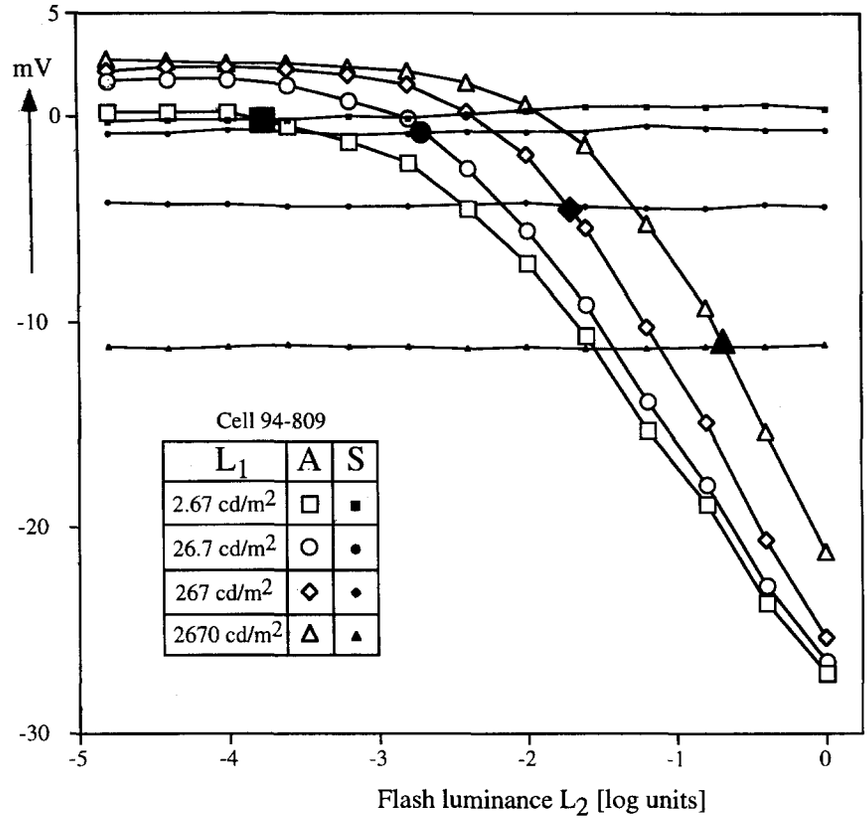

FIGURE 7. Graphical summary of the results illustrated in Fig. 6. Peak flash-response amplitude (A) in mV is plotted as a function of flash-luminance in log units. Flash luminance briefly replaces background luminance during a flash. Steps between the data points are 0.4 log units along the flash-luminance axis (abscissa). Background luminances and corresponding symbols are given in the inset. The larger filled symbols indicate the "operating point" as discussed in the text. Horizontal lines with small filled symbols, the data points, represent the measured hyperpolarization levels (*S*) with each of the four background luminances (of corresponding symbol form). Note that this level is hardly influenced by the flashes and only depends upon the background level. Dark flashes go to the left from the operating point and evoke responses in the upward direction, light flashes go to the right from the operating point and evoke hyperpolarizing responses indicated in the downward direction in this figure.

5(B) is highly similar to the curve that results if (A) is flipped vertically (mirrored in a horizontal axis), that is to the sensitivity (=1/threshold) as a function of background luminance. To show this parallel between sustained potential level and threshold (or its inverse) more directly we plotted the flash threshold as a function of the sustained potential level in Fig. 5(C and D). The former panel refers to relatively small test flashes on a relatively large background, where we expect that the flashes should not influence the sustained level very much. In Fig. 5(D) on the other hand we have varied the size of the background spot from the relatively large diameter of 8.6 deg down to the size of the small test spot (1.1 deg). Both threshold and sustained level change in a similar way with background spot-size, which supports the suggestion of a direct relation between the two, or a common cause. To further test this hypothesis we analysed data from a third type of experiment, described below.

Experiment 3

If there is a strong coupling between hyperpolarization level and gain one might wonder whether this also holds for decrements rather than only increments as studied in the previous experiment. Experiment 3 is an attempt to answer this question. Equal-sized spots S_1 and S_2 (dia 3.1 deg) of different luminance L_1 and L_2 are instantly exchanged at the same position. If S_1 is on for a relatively long period it acts as "background" and sets the adaptation level. If subsequently S_2 briefly replaces S_1 the result is a dark or a light flash or no stimulus, depending upon the values of L_1 and L_2. This is our usual way to generate both dark and light flashes with the optic set-up of Xenon light sources and fast shutters (opening and closing times < 1 msec). Results of such an experiment on H-cells look like the example recordings superimposed in Fig. 6. The four panels present results for the four background levels, that is spot S_1 having a luminance L_1 of -3.0, -2.0, -1.0 and 0 log units, where 0 log units equals 2670 cd/m^2. In this set-up the "test" channel (S_2 with luminance L_2) and "background" channel differ about a log unit in maximum luminance output (actually 0.95 log units): for L_2 0 log units equals 15900 cd/m^2. To prevent confusion we will give the background in cd/m^2 and only the test flash in log units.

At the highest background light level in the right hand panel we see almost symmetrical responses to increments and decrements, both with an overshoot at on and off.

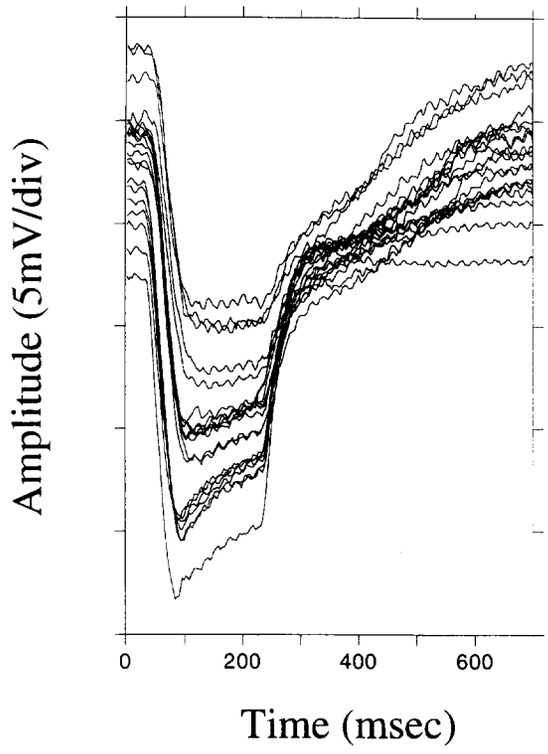

FIGURE 8. Superimposed threshold-flash responses for white light measured at (about) 1 min intervals during dark adaptation after a 10 sec pre-adaptation to an 8.8 deg dia spot of 6310 cd/m^2. These responses fulfilled a high threshold criterion (13 mV), which was chosen in this case to bring out the RAE more clearly. The threshold measurement procedure is described in the text. The RAE increases gradually during dark adaptation, so the responses with the largest slow after-potentials are measured later, after about 20 min of dark adaptation. The hyperpolarization level decreased gradually during dark adaptation.

The sustained polarization level leaves sufficient room in the depolarization direction for strong dark-flash responses. Going to the left in Fig. 6 we see that the available range in the depolarization (=decreasing hyperpolarization) direction decreases for lower background levels and that this appears to correlate with an upward shift of the baseline hyperpolarization level. There appears to be a fixed ceiling and thus the higher the baseline polarization level in Fig. 6 the less scope for responses in the upward (less hyperpolarizing) direction. The rod aftereffect (RAE), first analysed in detail for cat H-cells by Steinberg (1969), only appears for the most intense flashes on the lower background levels in Fig. 6. The responses of this H-cell are strongly cone-dominated for the range of 3 log units displayed in the figure. To get a better feeling for the relation between the peak response-amplitudes for dark and light flashes and the baseline polarization level a more quantitative summary of the results is presented in Fig. 7.

The horizontal lines with the small filled symbols represent the baseline (hyperpolarization) levels for the four different background intensities. Note that we do not know the absolute value of the hyperpolarization at the beginning of the recording, so we arbitrarily define the starting level (background spot switched off) as 0 mV. From the start of the recording onwards we can track the polarization level very precisely relative to this arbitrary zero level. Thus, all curves and lines in Fig. 7 are positioned accurately relative to each other, the scale intervals on the ordinate are correct but the choice of the origin (zero) on the ordinate is arbitrary. Where the horizontal lines of baseline polarization level cut their corresponding flash-amplitude curve we find the "operating point", marked with large filled symbols. The corresponding "flash luminance" is the zero flash for that operating point, the exchange-flash intensity that equals the background intensity. From that zero-flash point luminances to the left represent dark-flashes, luminances to the right light-flashes. Due to technical limitations the highest possible exchange-flash intensity was 15 900 cd/m^2 with which we could not explore the limit of the hyperpolarization range at the higher background intensities (triangles and diamonds). Only for the lower backgrounds do we see a slight tendency of the hyperpolarization level to level off for the strongest flashes (circles and squares). On the other hand the limitations of the range in the other (depolarization) direction are clearly visible for all four background levels. For the lowest background (squares) there is hardly scope for dark responses, but a wide range for light responses. Going to higher backgrounds we see an increase of the range for dark responses and a decrease of the range for light responses. Given the relatively fixed upper and lower limits of the operating ranges, it is clear that the baseline polarization level, the position of the operating point on the flash response curves, is of major importance. Figure 6 shows that the overshoots at on and at off are stronger for larger excursions relative to the set-point (=left-most or right-most point on the traces), both for the depolarizing and the hyperpolarizing directions. The relation between background luminance and set-point is again nonlinear, as already found in Fig. 5 and as expected from the model in Fig. 1. The slight upward shift in Fig. 7 of the ceiling of the curves with increasing background luminance is a consequence of the positive-going overshoots in response to the dark flashes that can be seen in Fig. 6. Although Fig. 7 gives a clear illustration of the importance of the hyperpolarization level in setting limits to both light and dark flashes it is less suitable to estimate the gain, since that requires plotting the flash amplitude relative to the background, rather than the exchange-flash luminance itself. Doing so gives results similar to those of Experiment 2.

Experiment 4

The final experiment was a prolonged dark adaptation of H-cells. After impalement, centering of the light spot on the RF (first roughly by hand and then with an automatic procedure), a series of initial measurements was performed. These included RF size measurements, DeLange curves and *R–I* curves. Just before dark adaptation, the cell was light adapted for 10 sec to an 8.8 deg spot of 3.8 log cd/m^2. After switching off this

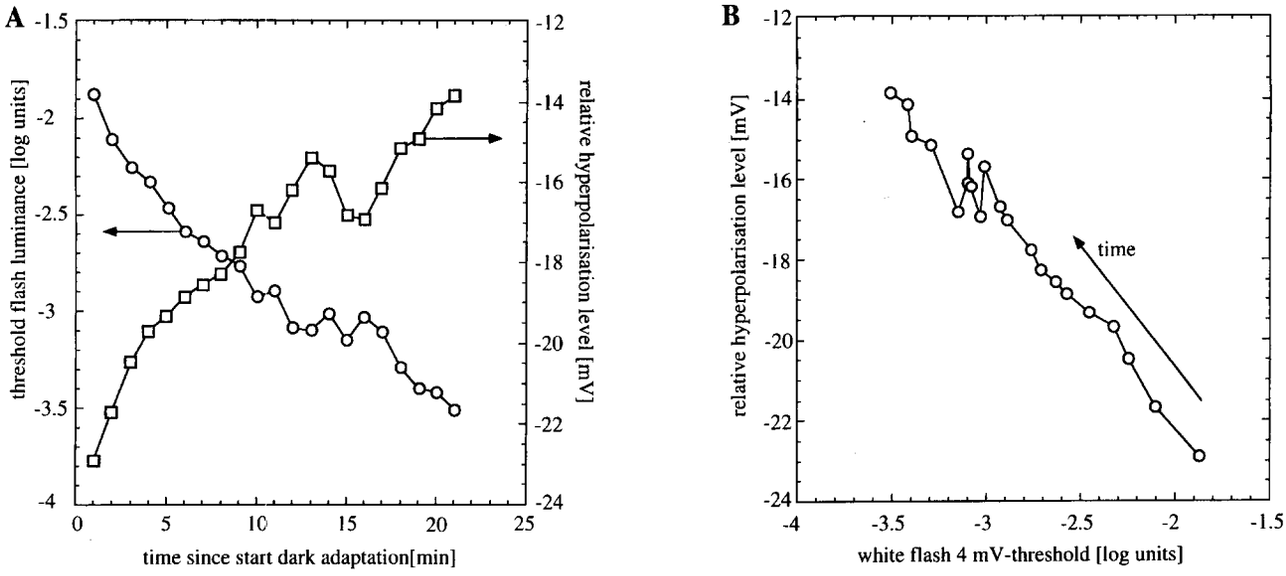

FIGURE 9. H-cell thresholds and sustained membrane potential plotted as a function of time since the start of dark adaptation. (A) ○, Indicate the threshold flash luminance as a function of time (measured with 1 min intervals) and the corresponding vertical axis is given to the left. □, relative hyperpolarization level in mV as indicated on the corresponding vertical axis to the right. Hyperpolarization is measured relative to that at the start of the recording which is arbitrarily called 0. Note how hyperpolarization level and threshold mirror each other, even during fluctuations. In (B) hyperpolarization at time t is plotted against log threshold-luminance at time t, where the time t since the start of dark adaptation increases, as indicated by the arrow, in 1 min steps.

adaptation stimulus the retina was allowed to dark adapt. Thresholds for 200 msec flashes of white light, 503 nm narrow-band light and 583 nm narrow-band light were measured every minute [see Lankheet *et al.* (1996a), for precise characteristics of the interference filters used to make these rod-preferred and cone-preferred light stimuli]. The threshold was determined by increasing the flash intensities in 0.4 log unit steps, starting from a level 2.0 log units below the estimated threshold, until a threshold-criterion (usually 3 or 4 mV, sometimes higher) was met. The interval between subsequent flashes was 2 sec. Figure 8 illustrates a superimposed series of white-light threshold-responses measured with (about) 1-min intervals. Here the threshold-criterion was 13 mV to bring out the cone response. For lower criterion threshold-responses the rod-component dominates (not shown). The on-response starts from an adaptation-dependent level and has an on-amplitude that is roughly constant. [At first sight accuracy might appear to be limited by the choice of 0.4 log unit intensity-steps for the flash control, but in fact interpolation allows higher precision: Lankheet *et al.* (1996a)]. This on-response appears to be cone-dominated and constant throughout the process of dark adaptation for the chosen high threshold-criterion. The variable slow part of the response is the rod contribution, which becomes best visible after the fast cone contribution has disappeared at light-off. The remaining slow RAE increases in amplitude during dark adaptation and appears to add to the baseline hyperpolarization level.

To get a better perspective on the relation between threshold and baseline hyperpolarization both are plotted as a function of time since the start of dark adaptation in Fig. 9(A). It can be seen that the white-flash threshold (left-hand vertical axis) decreases steadily with time in the dark. The hyperpolarization level relative to the membrane potential at the beginning of the recording (right-hand vertical axis) increases during dark adaptation, that is, the cell hyperpolarizes less and less as time goes by. Figure 9(A) suggests already that there is a strict coupling between the H-cell repolarization in the dark and the threshold-decrease (gain change). This is even more clearly shown in Fig. 9(B) where the relative hyperpolarization values are plotted against the white-flash thresholds that are measured at the same time. Time increases in the direction of the arrow. It can be seen that log threshold and relative hyperpolarization are tightly coupled as would be expected for models of the type as sketched in Fig. 1. Note also in Fig. 9(A) how even fluctuations in threshold and hyperpolarization level mirror each other faithfully.

Despite this nice concordance we must emphasize that the model in Fig. 1 was not designed to reproduce the slow process of dark adaptation and thus does not mimic it. The only thing we have established is an apparently rather strict coupling between increment/decrement sensitivity and the hyperpolarization level, and that this holds both in light and dark adaptation. Still this is interesting since it means that it holds for cone as well as rod contributions. From results such as those in Fig. 8 we could determine the rod contribution to the H-cell response. It appeared to grow from virtually 0 mV at the beginning of dark adaptation to about a maximum of 8–12 mV after 30 min or more of dark adaptation. The

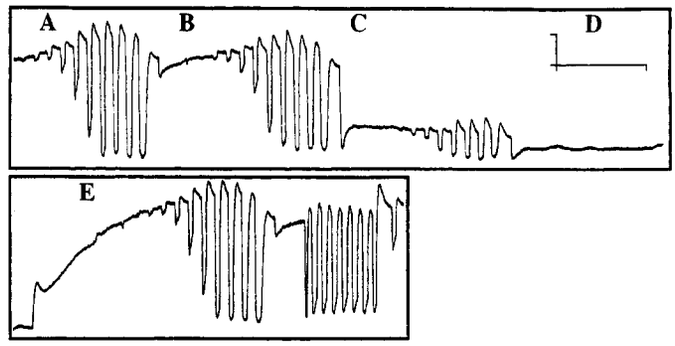

FIGURE 10. Light adaptation behaviour of a purely rod-driven HBAT (HB-cell axon terminal). It illustrates rod saturation and delayed off-responses to saturating flashes, which are visible as a lengthening of the response duration. Test flashes of 400 msec were delivered with an 800 msec interval and had a luminance increasing in 0.4 log unit steps from left to right in the illustration. Lowest flash luminance 0.16 cd/m^2 and highest flash luminance 1585 cd/m^2. Background luminances: 2.67 cd/m^2 in (A and E), 26.7 cd/m^2 in (B), 267 cd/m^2 in (C) and 2670 cd/m^2 in (D). The latter background fully saturates the rods so that they cannot respond to the flashes. Vertical calibration bar represents 2 mV, the horizontal bar 10 sec.

rod-response range appeared to add to a more-or-less fixed cone-response range, thus enlarging the maximally possible amplitude of H-cell light-responses from about 35 to about 45–47 mV after prolonged dark adaptation. It should be stressed, however, that the flash-intensities necessary to get a measurable rod-response in H-cells are at least 2 log units higher than the absolute threshold in dark adapted (and thus rod-dominated) G-cells. The rod contribution can then still be measured for weak flashes in G-cells, but not in H-cells. As soon as a stronger flash is delivered, the rod–cone gap junctions appear to open very fast, because the rod-response then becomes immediately measurable in H-cells. One possibility is that these gap junctions open whenever the connected rods are hyperpolarized more strongly by a certain amount than the cone.

As stated in the introduction, it is harder to get the extremely stable recordings from HBATs that are necessary to follow their dark adaptation process. These units are easily recognized from their responses to light and we have obtained several reasonably stable recordings at low-photopic and high-mesopic adaptation levels. The HBAT directly mirrors many of the characteristics that are customarily attributed to rods. At sufficiently high background levels their response to flashes or flicker is completely suppressed, as we expect holds for rods under these circumstances, the so-called rod-saturation. An example of an HBAT-recording is presented in Fig. 10 to illustrate why we think it is reasonable to postulate that the slower humps in the off-responses of Figs 8 and 6 are due to the delayed recovery of rods. The recordings in Fig. 10 stem from a unit that behaved exactly like the few HBATs that we were able to stain and recognize from histological examination. In Fig. 10(A–D) we present responses to flashes increasing from -0.8 to 3.2 cd/m^2, in steps of 0.4 log units on backgrounds of 2.67 cd/m^2 (A), 26.7 cd/m^2 (B), 267 cd/m^2 (C) and 2670 cd/m^2 (D). After this the background is switched back to 2.67 cd/m^2 in Fig. 10(E), where another series of flashes is given.

It is clear from Fig. 10 that the rods are completely saturated at the highest of these background intensities [Fig. 10(D)] and that their response range has both a fixed minimum and a fixed maximum hyperpolarization level. No light-responses can be evoked if the hyperpolarization level has reached the maximum of its range. The rod signal appears to be clamped at that level. For example, in Fig. 10(D) the flashes do not evoke any discernable reaction at all. Even at low backgrounds as in Fig. 10(A and E) the light-response can apparently never pass this fixed limit to hyperpolarization. Flashes stronger than necessary to just reach this maximum hyperpolarization lead to lengthening of the response, which is visible in Fig. 10(A–C) and Fig. 10(E) for the strongest flashes of the series. This phenomenon has the same origin as the RAE that we see in mixed-input H-cells after rod saturation. It appears that this fixed maximum hyperpolarization is at the same time the saturation level of rods, where they are clamped as soon as light levels are too high. After the switch from Fig. 10(D) to Fig. 10(E) one can see the rod contribution slowly recover to the more dark adapted situation [Fig. 10(E)], where the response is similar to that in Fig. 10(A) (same background luminance of 2.67 cd/m^2). This slow recovery, if seen in combination with a fast initial transient due to cones in mixed-response H-cell bodies, is a component of the RAE.

DISCUSSION

Steinberg (1969) in an important and careful study of rod contributions to cat H-cell responses states that the RAE appears unrelated to the recovery of either cone or rod excitability and that H-cell responses return to baseline long before excitability recovers (p.1349). Our present results seem to be in conflict with these statements. We find that H-cell sensitivity is tightly coupled to the resting membrane potential (hyperpolarizing level) under photopic as well as scotopic conditions. However, Steinberg also mentions that his recordings were not always optimally stable and could certainly not be held for longer than about 20 min. We think a relation

between hyperpolarization level and sensitivity, RAE and polarization-limits can only be deduced from extremely stable recordings where the hyperpolarization level shows no light-independent drift at all. Also in our experiments we often penetrate cells from which we can record very well up to, say, 20–30 min and where we nevertheless cannot get the recording completely drift-free. Their flash and flicker responses look normal, even for low temporal frequencies, but the recording baseline shows drift. We assume that this is a sign of imperfect sealing between the electrode and the penetrated membrane. With small leakage the potential modulations are apparently less strongly affected than the DC-component. In the present study we had quite a few cells that were extremely stable even for recording periods of several hours, with no deterioration of the light responses and a drift-free hyperpolarization level. Such recordings provide a different view of gain control mechanisms and suggest that the baseline membrane potential might play a role in setting operating points, gains and time constants, possibly as proposed in models like the one in Fig. 1. For cyprinid fish H-cells (Naka & Rushton, 1968) and skate H-cells (Dowling & Ripps, 1970), it was reported that there was no apparent relation between hyperpolarization level and (log) sensitivity. In view of the mentioned drift problem we think these negative findings cannot be taken at face value. This interpretation is supported by results of Grabowsky *et al.* (1972) who recorded from axolotl red rods and found that most recordings showed random drift. In only two exceptionally stable drift-free recordings they found that the repolarization of the rods after bleaching paralleled the log threshold decrease for up to 15–20 min. Similar findings are more numerous in modern work.

In fact the rod responses reported by Grabowsky *et al.* (1972) appear to adapt and saturate in a way that is qualitatively quite similar to the behaviour of our H-cell rod-component (Lankheet *et al.*, 1996a). The results of Tamura *et al.* (1989) on cat rods support the idea that there is a high degree of similarity between adaptational properties of cat rods and those of many lower vertebrate species. Taken together this means that the coupling found above between hyperpolarization level of H-cells and their flash-sensitivity during dark adaptation (Fig. 9) might stem from a coupling between these parameters in the rods. However, since the rod component enters the H-cell through cones it would also have to adapt in a cone-like manner, that is the gain of the H-cell's rod component should be the product of rod gain, rod–cone gap-gain, cone gain and H-cell gain. It remains to be seen how well such a model would work.

Yang and Wu (1989) studied the influence of background illumination on H-cell responses in the tiger salamander retina and found that the rise time of H-cell flash responses did not correlate well with the H-cell hyperpolarization level. This conflicts with our findings for the cat and might be a species difference. On the whole the H-cell flash-response waveforms shown in their paper (especially their Figs 6 and 15) are of widely different shape compared to those in the cat, even after correction for the different time-scales due to different body temperatures of cat and salamander. Wu (1987b) reported that for any given resting potential value the rise time is much slower under dark-adapted than under light adapted conditions. In cat H-cells we cannot even obtain the same hyperpolarization level under dark adapted as under light adapted conditions, since the resting potential is representative of the state of adaptation. (Voltage-clamping could in principle be used to change this but would lead to an entirely different type of experiment and interpretation, as discussed in the next paragraph). These species differences are surprising in view of the H-cell responses reported by Wu (1987a), also for the salamander retina, which look very much more like time-scaled cat H-cell responses. Furthermore he reports that salamander H-cells appear to have approximately fixed limits for both depolarizing and hyperpolarizing voltage-changes, which seems quite compatible with our findings for the cat. Also the "voltage-tails" (RAEs) shown in that study and in Wu (1988) show a strong similarity to those in the cat. This parallel for the rod-component of H-cell responses in cat and salamander fits in with the strong similarity in properties of rods in mammals and other vertebrates mentioned in the previous paragraph.

The relation between hyperpolarization level and flash sensitivity has also been studied in turtle cones where a close correlation was found (Baylor & Hodgkin, 1974; Copenhagen & Green, 1985, 1987; Itzhaki & Perlman, 1987). A flash-sensitivity reduction by a factor $1/e$ (0.368) roughly corresponded to a 3 mV hyperpolarization change. If a similar fixed relation would also prove to hold for cat cones it would open the possibility that the relation found above for light-adapted H-cells in the cat simply reflects a tight coupling between polarization level and sensitivity in cones. For our model of Fig. 1 this could mean that most of the components should be viewed as parts of a cone-model. Green *et al.* (1994) tested the hypothesis that membrane polarization in cones of the turtle could somehow control flash sensitivity by using extrinsic currents to manipulate the membrane potential independent from light stimulation. They found that extrinsic hyperpolarizing current indeed reduced the amplitude and time to peak of the flash response (as our model would suggest). However, unlike background-light extrinsic current did not affect the time-course of the falling phase of the response. Moreover, extrinsic current and background light had different effects on the intensity-response function. Green *et al.* (1994) concluded that hyperpolarization cannot in itself adapt the cone-response in the same way that light does. We concur with this general conclusion. However, a quantitative assessment of the role of the membrane potential (if any) in setting flash sensitivity first of all requires a better specification of the presumed transformation from light to membrane potential. For example, even in a simple model as in Fig. 1 it is clear that light and membrane currents will not have exactly the same influence if we

assume that the scale-factor setting is done in a synapse or by some chemical (not voltage-controlled) process internal to a cone or an H-cell. In that case the process cannot be assumed to run exactly the same in the reverse direction as in the forward direction. One would only expect that membrane currents and light have a similar influence on the scale-factor if it is controlled by the membrane-voltage (or current).

The results of our dark adaptation studies suggest that the rod-component's operating range is added to that of the cone in H-cell responses and that this is inconsequential as soon as the rods are saturated. The rod contribution not only changes sensitivity by shifting its *R–I* curve along the intensity axis, as holds for the cone contribution, but it also changes its range (V_{max}) with adaptation level (saturation). This is incorporated in a simple but adequate description of our dark adaptation results for H-cells by Lankheet *et al.* (1996a). In that paper we showed that a good fit to the data is obtained if one assumes independent adaptation of rods and cones and summation of their signals in H-cells. In rods the (*R–I*) operating curves shift about 3 decades horizontally to lower intensities and expand in voltage range from 0 (saturation) to about 12 mV during prolonged dark adaptation, whereas the cone operating curves shift about 1 decade horizontally and do not change in range. The operating points σ of both rods and cones change exponentially with time during dark adaptation from a light adapted value to a lower dark adapted value. To incorporate dark adaptation in our model it would thus indeed be sensible to place all of the adaptation and saturation machinery in the rods and cones and model the H-cell as a simple summator and filter. The model of Fig. 1 would thus become a cone-model, and we would have to develop a separate rod-model and formulate additional postulates regarding the spatial interactions. In this respect our finding (Lankheet *et al.*, 1996b) that the spatial summation properties of H-cells also change during dark-adaptation shows that it would be imperative to include H-cell coupling by gap junctions in the model. Since rod signals are not visible in H-cell bodies at scotopic luminances but must be assumed to be available to BR-cells it seems reasonable to assume that the rod–cone gap junctions close at low luminances (starting about two decades above the absolute threshold for G-cells). On the other hand the increase in H-cell RF sizes measured at their dark adapted level relative to those in light adapted situations suggests that the gap junctions between H-cell bodies get a lower resistance during dark adaptation. Thus cat H-cell bodies seem to be more tightly coupled, but rods seem to decouple from cones in the scotopic range. For the white perch Tornqvist *et al.* (1988) report that cone-driven H-cells have a decreasing RF-size during dark adaptation. For the carp Yang *et al.* (1994) find that these cells give a decreasing flash response during dark adaptation (dark suppression). Both these findings are exactly the opposite of what we found for (cone dominated) cat H-cell bodies! However, it should be added that it is not difficult to find reports for lower vertebrates that are more in line with our findings for the cat. For example, Dong and McReynolds (1992) report for mudpuppy H-cells that both flickering light and steady background light decrease H-cell RF-size, that is uncouple H-cells, probably through dopamine release by on-pathway cells. Similar results were reported for turtle H-cells by Weiler and Akopian (1992). We are at a loss to explain such discrepancies, but they illustrate how hazardous it is to assume that findings for one species also hold for another.

Results such as those in Fig. 10 show that, due to rod saturation, the rod contribution to H-cell light responses disappears for photopic background levels. This phenomenon of rod saturation was first discovered in human psychophysics by Stiles in 1939 [e.g. see Aguilar & Stiles (1954)]. Daw and Pearlman (1971) studied it in cats with the help of extracellular recordings in the LGN. They measured thresholds for light spots as a function of the background luminance and found that an initially linear relation between log increment-threshold and log background-luminance saturated after a few log units increase of the background, leading to a virtually infinite threshold for rod stimuli. For appropriate wavelengths of the test stimuli the L-cones (555–560 nm cones) then took over. Adelson (1982) has developed a gain-control model of rod saturation that is similar in spirit to the type of model drawn in Fig. 1 and that would seem to comply with the findings of Daw and Pearlman (1971). It might be used as the basis of a rod model to be included with the extended H-cell network-model outlined above. Foerster *et al.* (1977a, b) also proposed to add the rod signal to that from cones right at the input of the H-cell model. They included the required compression nonlinearity in the H-cell, but it could in principle also be part of the receptor models. Taken together we think most of the boundary conditions for a reasonably complete systems model of H-cell functioning are now available.

Our findings also support proposals by Smith *et al.* (1986), Sterling *et al.* (1986, 1988), Wässle *et al.* (1991) and others, that the separate rod pathway from BR-cell (rod bipolar)→AII-cell→BC-cells (cone bipolars)→G-cells is more light-sensitive than the alternative route R→C→H→ etc. The latter pathway for rod signals was discovered by Nelson (1977) who found rod signals in cones and explained them by the gap junctions between cones and rods. This pathway via the cones betrays its properties in HA- and HB-cell (soma) recordings. The BR to AII pathway on the other hand is responsible for G-cell responses to rod signals at light levels two or possibly more decades below the threshold for rod contributions in H-cell bodies. The relatively high absolute light threshold of H-cell soma-responses characterizes them as mesopic/photopic cells. Even after 45 min of dark adaptation we never found even the slightest trace of quantum noise in H-cell soma-recordings and their thresholds stayed high (Lankheet *et al.*, 1996a,b). If H-cell bodies are responsible for the RF surround of G-cells, this predicts that the mixed cone-rod surround disappears a few log units above the absolute threshold for G-cells. It may be, but

remains unproven, that HBATs then take over and provide an all-rod RF surround (via BR-cells). A separate low-luminance gain control in the proximal layers of the retina, as proposed a.o. by Frishman and Sieving (1995), is a serious alternative since BR-cells do not appear to have a centre–surround organization. Photopic and high-mesopic gain control would then take place at the outer plexiform layer, with a prominent role for the receptors and H-cells, whereas scotopic gain control would take place at more proximal sites. The scotopic threshold response (STR) studied by Sieving *et al.* (1986), Steinberg *et al.* (1991) and others is a response that can be eliminated by backgrounds that are so weak that they have no influence on the PII-wave of the ERG, do not adapt rod outer segments nor H-cell bodies. Thus there appears to be a network in control of scotopic adaptation in the proximal retina. This division of labour between outer plexiform layer (photopic adaptation networks) and proximal retina fits with our finding that H-cell bodies have no interest whatsoever in scotopic processes. However, the role of HBATs then remains even more mysterious. Their RFs are much larger than those of BR-cells (3000 vs 15–40 rod inputs). Therefore, if they set the gain of rods by feedback-control this would have to be some form of shunting inhibition that does not show up in a centre–surround structure of BR-cells.

In conclusion, we have presented a model and data on gain control processes in the outer plexiform layer and found that H-cell bodies do not play a role in scotopic vision since they are a factor of 100 or more less sensitive to light flashes than G-cells. H-cells do show dark adaptation, however, and during dark adaptation the rod component increases, whereas the cone component does not or only very little. The voltage range available to rod responses grows with dark adaptation and is added to the cone range in H-cell bodies. The baseline hyperpolarization level correlates very well with flash sensitivity and might be one of the control variables of sensitivity. Alternatively the correlation might stem from a common cause, e.g. a similar strong correlation in the cones and in the rods as found for other species. The finding that (a) symmetry between dark and light flash responses in H-cell bodies depends among other things on flash duration (Fig. 3) could inspire psychophysical work in humans. Moreover, the arguments of this discussion suggest that this asymmetry might stem from scaling actions in the receptors, a prediction that seems worth testing. Since the original model of H-cells mimicked the dynamic properties of H-cells so well (Lankheet *et al.*, 1993b), it might be worthwhile to modify it as detailed above. The feedback-scaler might have to be placed in the cones and should there be preceded by the time-constant-adaptation network. A separate rod-model should be developed [similar to that of Adelson (1982)], the output of this rod model should be added (via a gap-junction model) to the cone model which should synapse on the H-cell membrane. Since lateral couplings between H-cells and between rods and cones should also be taken into account, as well as the slow process of dark adaptation, the next step in the model-evolution is certainly nontrivial and needs to be left to future work.

REFERENCES

Adelson, E. H. (1982). Saturation and adaptation in the rod system. *Vision Research, 22*, 1299–1312.

Aguilar, M. & Stiles, W. S. (1954). Saturation of the rod mechanism of the retina at high levels of stimulation. *Optica Acta, 1*, 59–65.

Baylor, D. A. & Hodgkin, A. L. (1974). Changes in time scale and sensitivity in turtle photoreceptors. *Journal of Physiology, 242*, 729–758.

Bouman, M. A. & Ampt, C. G. F. (1966). Fluctuation theory in vision and its mechanistic model. In Bouman, M. A. & Vos, J. J. (Eds), *Performance of the eye at low luminances* (pp. 57–69). Excerpta Medica Int. Congr. Series, No. 125.

Bouman, M. A., van de Grind, W. A. & Zuidema, P. (1985). Quantum fluctuations in vision. *Progress in Optics, XXII*, 79–144.

Brown, K. T. & Flaming, D. G. (1977). New microelectrode techniques for intracellular work in small cells. *Neuroscience, 2*, 813–827.

Copenhagen, D. R. & Green, D. G. (1985). The absence of spread of adaptation between rod photoreceptors in turtle retina. *Journal of Physiology, 369*, 161–181.

Copenhagen, D. R. & Green, D. G. (1987). Spatial spread of adaptation within the cone network of turtle retina. *Journal of Physiology, 393*, 763–776.

Daw, N. W., Jensen, R. J. & Brunken, W. J. (1990). Rod pathways in mammalian retinae. *TINS, 133*, 110–115.

Daw, N. W. & Pearlman, A. L. (1971). Rod saturation in the cat. *Vision Research, 11*, 1361–1364.

Dong, C.-J. & McReynolds, J. S. (1992). Comparison of the effects of flickering and steady light on dopamine release and horizontal cell coupling in the mudpuppy retina. *Journal of Neurophysiology, 672*, 364–372.

Dowling, J. E. & Ripps, H. (1970). Visual adaptation in the retina of the skate. *Journal of General Physiology, 56*, 491–520.

Foerster, M. H., van de Grind, W. A. & Grüsser, O.-J. (1973). Intracellular recordings from different layers of the cat retina. *Pflügers Archiv für die gesammte Physiologie, 343*, Suppl. 180.

Foerster, M. H., van de Grind, W. A. & Grüsser, O.-J. (1977a). Frequency transfer properties of three distinct types of cat horizontal cells. *Experimental Brain Research, 29*, 347–366.

Foerster, M. H., van de Grind, W. A. & Grüsser, O.-J. (1977b). The response of cat horizontal cells to flicker stimuli of different area, intensity and frequency. *Experimental Brain Research, 29*, 367–385.

Frishman, L. J. & Sieving, P. A. (1995). Evidence for two sites of adaptation affecting the dark-adapted ERG of cats and primates. *Vision Research, 35*, 435–442.

Gaudiano, P. (1994). Simulations of X and Y retinal ganglion cell behavior with a nonlinear push–pull model of spatiotemporal retinal processing. *Vision Research, 34*, 1767–1784.

Grabowsky, S. R., Pinto, L. H. & Pak, W. L. (1972). Adaptation in retinal rods of Axolotl: Intracellular recordings. *Science, 176*, 1240–1243.

Green, D. G., Schneeweis, D. M. & Glover, M. J. (1994). Extrinsic current and flash sensitivity in turtle cones. *Vision Research, 34*, 429–435.

van de Grind, W. A. (1981). Intracellular recording studies of visual signal processing in the cat retina. In Maffei, L. (Ed.), *Pathophysiology of the visual system. Doc. Ophthal. Proc. Series 30*, (pp. 21–30). The Hague: Junk Publ.

van de Grind, W. A. & Grüsser, O.-J. (1981). Frequency transfer properties of cat retina horizontal cells. *Vision Research, 21*, 1565–1572.

van de Grind, W. A., Grüsser, O.-J. & Lunkenheimer, H.-U. (1973). Temporal transfer properties of the afferent visual system: Psychophysical, neurophysiological and theoretical investigations.

In Jung, R. (Ed.), *Handbook of sensory physiology* Vol. VII/3A (Central Processing of Visual Information) (Chap. 7, pp. 431–573). Berlin: Springer.

van de Grind, W. A., Koenderink, J. J., van der Heyde, G. L., Landman, H. A. A. & Bouman, M. A. (1971). Adapting coincidence scalers and neural modelling studies of vision. *Kybernetik, 8*, 85–105.

Grüsser, O.-J. (1957). Rezeptor Potentiale einzelner retinaler Zapfen der Katze. *Naturwissenschaften, 44*, 522.

Itzhaki, A. & Perlman, I. (1987). Light adaptation of red cones and L1-horizontal cells in the turtle retina: Effect of the background spatial pattern. *Vision Research, 27*, 685–696.

Kolb, H. & Nelson, R. (1984). Neural architecture of the cat retina. *Progress in Retinal Research, 3*, 21–60.

Lankheet, M. J. M., Frens, M. A. & van de Grind, W. A. (1990). Spatial properties of horizontal cell responses in the cat retina. *Vision Research, 309*, 1257–1275.

Lankheet, M. J. M., Molenaar, J. & van de Grind, W. A. (1989a). The spike generating mechanism of cat retinal ganglion cells. *Vision Research, 29*, 505–517.

Lankheet, M. J. M., Molenaar, J. & van de Grind, W. A. (1989b). Frequency transfer properties of the spike generating mechanism of cat retinal ganglion cells. *Vision Research, 29*, 1649–1661.

Lankheet, M. J. M., Prickaerts, J. H. H. J. & van de Grind, W. A. (1992). Responses of cat horizontal cells to sinusoidal gratings. *Vision Research, 32*, 997–1008.

Lankheet, M. J. M., Przybyszewski, A. W. & van de Grind, W. A. (1993a). The lateral spread of light adaptation in cat horizontal cell responses. *Vision Research, 33*, 1173–1184.

Lankheet, M. J. M., Rowe, M. H., van Wezel R. J. A. & van de Grind, W. A. (1996a). Horizontal cell sensitivity in the cat retina during prolonged dark adaptation. *Visual Neuroscience* (in press).

Lankheet, M. J. M., Rowe, M. H., van Wezel, R. J. A. & van de Grind, W. A. (1996b). Spatial and temporal properties of cat horizontal cells after prolonged dark adaptation. *Vision Research, 36*, 3955–3967.

Lankheet, M. J. M., van Wezel, R. J. A. & van de Grind, W. A. (1991a). Effects of background illumination on cat horizontal cell responses. *Vision Research, 31*, 919–932.

Lankheet, M. J. M., van Wezel, R. J. A. & van de Grind, W. A. (1991b). Light adaptation and frequency transfer properties of cat horizontal cells. *Vision Research, 31*, 1129–1142.

Lankheet, M. J. M., van Wezel, R. J. A., Prickaerts, J. H. H. J. & van de Grind, W. A. (1993b). The dynamics of light adaptation in cat horizontal cell responses. *Vision Research, 33*, 1153–1171.

Mangel, S. C. (1991). Analysis of the horizontal cell contribution to the receptive field surround of ganglion cells in the rabbit retina. *Journal of Physiology, 442*, 211–234.

Mangel, S. C. & Miller, R. F. (1987). Horizontal cells contribute to the receptive field surround of ganglion cells in the rabbit retina. *Brain Research, 414*, 182–186.

Molenaar, J. & van de Grind, W. A. (1979a). A visual stimulator for orbiting light spots and equal energy annuli with continuously variable parameters. *Experimental Brain Research, 37*, 65–71.

Molenaar, J. & van de Grind, W. A. (1979b). Anisotropic receptive field structure of cat horizontal cells. *Experimental Brain Research, 37*, 253–263.

Molenaar, J. & van de Grind, W. A. (1980). A stereotaxic method of recording from single neurons in the intact *in vivo* eye of the cat. *Journal of Neuroscience Methods, 2*, 135–152.

Molenaar, J., van de Grind, W. A. & Eckhorn, R. (1983). Dynamic properties of cat horizontal cell light responses. *Vision Research, 23*, 257–266.

Molenaar, J., Voorhorst, R., Schreurs, A. W., Broekhuyzen, P., Nivard, J. & van de Grind, W. A. (1980). A mechanical oscilloscope for vision research. *Pflügers Archiv, 383*, 173–179.

Motokawa, K., Oikawa, T. & Tasaki, K. (1957). Receptor potential of vertebrate retina. *Journal of Neurophysiology, 20*, 186–199.

Naka, K.-I. (1971). Receptive field mechanism in the vertebrate retina. *Science, 171*, 691–693.

Naka, K.-I. (1977). Functional organization of catfish retina. *Journal of Neurophysiology, 40*, 26–43.

Naka, K.-I. & Nye, P. W. (1971). Role of horizontal cells in organisation of the catfish retinal receptive field. *Journal of Neurophysiology, 34*, 785–801.

Naka, K.-I. & Rushton, W. A. H. (1968). S-potential and dark adaptation in fish. *Journal of Physiology (London), 194*, 259–269.

Naka, K.-I. & Witkovsky, P. (1972). Dogfish ganglion cell discharge resulting from extrinsic polarization of the horizontal cells. *Journal of Physiology, 223*, 449–460.

Nelson, R. (1977). Cat cones have rod input: A comparison of the response properties of cones and horizontal cell bodies in the retina of the cat. *Journal of Comparative Neurology, 172*, 109–134.

Nelson, R. & Kolb, H. (1983). Synaptic patterns and response properties of bipolar and ganglion cells in the cat retina. *Vision Research, 23*, 1183–1195.

Nelson, R., Kolb, H., Robinson, M. M. & Mariani, A. P. (1981). Neural circuitry of the cat retina. *Vision Research, 21*, 1527–1536.

Przybyszewski, A. W., Lankheet, M. J. M. & van de Grind, W. A. (1993). Nonlinearity and oscillations in X-type ganglion cells of the cat retina. *Vision Research, 33*, 861–875.

Przybyszewski, A. W., Lankheet, M. J. M. & van de Grind, W. A. (1995). Irregularities in spike trains of cat retinal ganglion cells. In Ditto, W., Pecora, L., Shlesinger, M., Spano, M. & Vohra, S. (Eds), *Proc. 2nd Exp. Chaos Conf.* (pp. 218–225). Singapore: World Scientific.

Rushton, W. A. H. (1965). Visual adaptation. The 1962 Ferrier Lecture. *Proceedings of the Royal Society London B, 162*, 20–46.

Rushton, W. A. H. (1972). Light and dark adaptation. *Investigative Ophthalmology, 11*, 503–517.

Sieving, P. A., Frishman, L. J. & Steinberg, R. H. (1984). Scotopic threshold response of proximal retina in cat. *Journal of Neurophysiology, 56*, 1049–1061.

Smith, R. G., Freed, M. A. & Sterling, P. (1986). Microcircuitry of the dark-adapted cat retina: Functional architecture of the rod–cone network. *Journal of Neuroscience, 6*, 3505–3517.

Steinberg, R. H. (1969). The rod after-effect in S-potentials from the cat retina. *Vision Research, 9*, 1345–1355.

Steinberg, R. H., Frishman, L. J. & Sieving, P. A. (1991). Negative components of the electroretinogram from proximal retina and photoreceptor. *Progress in Retinal Research, 10*, 121–160.

Sterling, P., Freed, M. A. & Smith, R. G. (1986). Microcircuitry and functional architecture of the cat retina. *Trends in Neuroscience, 9*, 186–192.

Sterling, P., Freed, M. A. & Smith, R. G. (1988). Architecture of rod and cone circuits to the ON-beta ganglion cell. *Journal of Neuroscience, 9*, 623–642.

Svaetichin, G. (1953). The cone action potential. *Acta Physiologica Scandinavia, 106Suppl.*, 565–600.

Tamura, T., Nakatani, K. & Yau, K.-W. (1989). Light adaptation in cat retinal rods. *Science, 245*, 755–758.

Tornqvist, K., Yang, X.-L. & Dowling, J. E. (1988). Modulation of cone horizontal cell activity in the teleost fish retina. III. Effects of prolonged darkness and dopamine on electrical coupling between horizontal cells. *The Journal of Neuroscience, 8*, 2279–2288.

Troy, J. B., Oh, J. K. & Enroth-Cugell, Ch. (1993). Effect of ambient illumination on the spatial properties of the center and surround of Y-cell receptive fields. *Visual Neuroscience, 10*, 753–764.

Wässle, H., Yamashita, M., Greferath, U., Grünert, U. & Müller, F. (1991). The rod bipolar cell of the mammalian retina. *Visual Neuroscience, 7*, 99–112.

Weber, A. J. & Stanford, L. R. (1994). Synaptology of physiologically identified ganglion cells in the cat retina: A comparison of retinal X- and Y-cells. *Journal of Comparative Neurology, 343*, 483–499.

Weiler, R. & Akopian, A. (1992). Effects of background illuminations on the receptive field size of horizontal cells in the turtle retina are mediated by dopamine. *Neuroscience Letters, 140*, 121–124.

Werblin, F. S. & Dowling, J. E. (1969). Organization of the retina of the mudpuppy, *Necturus maculosis* II. *Journal of Neurophysiology, 32*, 339–355.

Wu, S. M. (1987a). Changes in response waveform of retinal horizontal cells during dark and light adaptation. *Vision Research, 27*, 143–150.

Wu, S. M. (1987b). Light-dependent synaptic delay between photoreceptors and horizontal cells in the tiger salamander retina. *Vision Research, 27*, 263–267.

Wu, S. M. (1988). Synaptic transmission from rods to horizontal cells in dark-adapted tiger salamander retina. *Vision Research, 28*, 1–8.

Yang, X.-L., Fan, T.-X. & Shen, W. (1994). Effects of prolonged darkness on light responsiveness and spectral sensitivity of cone horizontal cells in carp retina *in vivo*. *The Journal of Neuroscience, 14*, 326–334.

Yang, X.-L. & Wu, S. M. (1989). Effects of background illumination on the horizontal cell responses in the tiger salamander retina. *Journal of Neuroscience, 9*, 815–827.

Acknowledgement—This work was supported by the Life Sciences Foundation (SLW) of the Netherlands Organization for Scientific Research (NWO).